

## Temperature Effects on the Solvent-Dependent Deactivation of Singlet Oxygen

Rasmus Lybech Jensen, Jacob Arnbjerg, and Peter R. Ogilby\*

Center for Oxygen Microscopy and Imaging, Chemistry Department, Aarhus University, DK-8000, Århus, Denmark

Received March 2, 2010; E-mail: progilby@chem.au.dk

**Abstract:** Singlet molecular oxygen,  $O_2(a^1\Delta_g)$ , is an intermediate in a variety of oxygenation reactions. The reactivity of singlet oxygen in a given system is influenced, in part, by competitive solvent-dependent channels that deactivate singlet oxygen in a nonradiative process. It has long been considered that these deactivation channels depend only slightly on temperature. This conclusion has been incorporated into the accepted empirically derived model of electronic-to-vibrational energy transfer used to account for the effect of solvent on the lifetime of singlet oxygen,  $\tau_\Delta$ . The current study reveals that  $\tau_\Delta$ , in fact, can depend quite significantly on temperature in certain solvents (e.g.,  $D_2O$  and benzene- $d_6$ ). These results can have practical ramifications in studies of singlet oxygen reactivity. From a fundamental perspective, these data indicate that aspects of the model for nonradiative deactivation of singlet oxygen need to be re-evaluated.

### Introduction

The lowest energy excited electronic state of molecular oxygen, singlet oxygen,  $O_2(a^1\Delta_g)$ , is an important reactive intermediate in a wide range of systems. In particular, singlet oxygen can oxygenate organic molecules in characteristic reactions that differ from those of the triplet ground state of oxygen,  $O_2(X^3\Sigma_g^-)$ . These reactions not only make singlet oxygen a useful synthetic reagent,<sup>1,2</sup> they also define the important role that singlet oxygen plays in many biological systems.<sup>3–5</sup>

In a given system, the chemical reactions of singlet oxygen kinetically compete with processes wherein singlet oxygen is simply deactivated to generate  $O_2(X^3\Sigma_g^-)$ .<sup>6</sup> This deactivation can be the result of collision-dependent interactions with (1) another solute, a so-called “quencher” added to the system, and/or (2) solvent molecules. The overall rate constant for singlet oxygen removal,  $k_\Delta$ , can thus be expressed as a sum of bimolecular terms as shown in eq 1,

$$k_\Delta = k_{nr}[M] + k_r[M] + k_q[Q] + k_{rxn}[R] \quad (1)$$

where  $R$  and  $Q$  represent the chemical reactant and quencher, respectively, and  $M$  represents the solvent. The solvent-dependent deactivation terms are further subdivided into a nonradiative process,  $k_{nr}$ , and a radiative process,  $k_r$ . The latter corresponds to the  $O_2(a^1\Delta_g) \rightarrow O_2(X^3\Sigma_g^-)$  phosphorescence at  $\sim 1275$  nm. The reciprocal of the first-order rate constant  $k_\Delta$  defines the lifetime of singlet oxygen,  $\tau_\Delta$ .

The development of methods to monitor singlet oxygen by its 1275 nm phosphorescence in time-resolved solution-phase experiments initiated a  $\sim 20$  year period of intense activity in which values of  $k_\Delta$  were obtained from a plethora of systems.<sup>6</sup> Of particular interest were studies designed to elucidate how values of  $k_{nr}$  and  $k_r$  varied with the solvent. It is now well-established that both  $k_{nr}$  and  $k_r$  depend significantly on the solvent, each in their own way (i.e.,  $k_{nr}$  does not respond to changes in the solvent in the same way as does  $k_r$ ).<sup>6,7</sup> Moreover, the inequality  $k_{nr} \gg k_r$  is applicable for most solvents of practical consequence. As such, it is the nonradiative deactivation channel that defines the solvent contribution in the kinetic competition with a given reactant. Alternatively, in the absence of solutes added to a given system, it is the nonradiative deactivation channel that defines  $\tau_\Delta$ .

On the basis of a phenomenal amount of data, including the results of experiments that quantify the remarkable solvent H/D isotope effects on  $\tau_\Delta$ , a model of collision-dependent electronic-to-vibrational energy transfer evolved over the years to account for the effect of solvent on  $k_{nr}$ .<sup>6</sup> Included in this analysis was the notion that  $k_{nr}$  does not depend significantly on temperature.

In considering the published studies in which the effect of temperature on  $k_{nr}$  is examined, it is prudent to only consider data obtained from direct  $O_2(a^1\Delta_g) \rightarrow O_2(X^3\Sigma_g^-)$  phosphorescence experiments. Specifically, indirect studies based on trapping experiments, for example, involve other processes that could likewise depend on temperature and, as such, could confuse the issue at hand.

Early reports pointed to very small, if any, temperature effects on  $\tau_\Delta$  over a  $\sim 100$  °C range in acetone- $h_6$ , acetone- $d_6$ , methyl propionate, chlorobenzene,  $CHCl_3$ , and  $CDCl_3$ .<sup>8–10</sup> To our knowledge, the first indication of a pronounced temperature

- (1) Clennan, E. L.; Pace, A. *Tetrahedron* **2005**, *61*, 6665–6691.
- (2) Montagnon, T.; Tofi, M.; Vassilikogiannakis, G. *Acc. Chem. Res.* **2008**, *41*, 1001–1011.
- (3) Foote, C. S.; Clennan, E. L. In *Active Oxygen in Chemistry*; Foote, C. S., Valentine, J. S., Greenberg, A., Liebman, J. F., Eds.; Chapman and Hall: London, 1995; pp 105–140.
- (4) Davies, M. J. *Biochem. Biophys. Res. Commun.* **2003**, *305*, 761–770.
- (5) Ogilby, P. R. *Chem. Soc. Rev.* **2010**; DOI: 10.1039/B926014P.
- (6) Schweitzer, C.; Schmidt, R. *Chem. Rev.* **2003**, *103*, 1685–1757.

- (7) Ogilby, P. R. *Acc. Chem. Res.* **1999**, *32*, 512–519.
- (8) Ogilby, P. R.; Foote, C. S. *J. Am. Chem. Soc.* **1983**, *105*, 3423–3430.
- (9) Hurst, J. R.; Schuster, G. B. *J. Am. Chem. Soc.* **1983**, *105*, 5756–5760.

effect on  $\tau_{\Delta}$  came from data recorded in  $\text{CS}_2$  and, independently,  $\text{CDCl}_3$ .<sup>11</sup> These latter  $\text{CDCl}_3$  data [ $\tau_{\Delta}$  (+22 °C) = 9.4 ms,  $\tau_{\Delta}$  (−50 °C) = 13.1 ms] are clearly not consistent with earlier  $\text{CDCl}_3$  data<sup>9</sup> that had been recorded over an even larger temperature range [ $\tau_{\Delta}$  = 0.64 ms; temperature independent over the range −90 °C to +37 °C]. Several points need to be mentioned in this regard. First, it has independently been established that, in halogenated solvents such as chloroform, radical-mediated processes involving the solvent can play a role in photosensitized singlet oxygen systems.<sup>8,12</sup> As such, depending on the way a given experiment is performed in  $\text{CDCl}_3$ , one may indeed see pronounced differences in (a) the value of  $\tau_{\Delta}$ , and (b) the effect of temperature due to the presence of radical-derived species that can quench singlet oxygen. Moreover, in solvents where  $\tau_{\Delta}$  is greater than ~5 ms (e.g.,  $\text{CS}_2$ ,  $\text{CDCl}_3$ ), it is generally the case that a variety of bimolecular quenching channels (i.e.,  $k_{\text{q}}[Q]$  in eq 1) can now readily compete with the  $k_{\text{nr}}[M]$  term. These include the quenching of singlet oxygen by the sensitizer and by ground state oxygen.<sup>11,13</sup> Thus, under these conditions, any observed temperature effect on  $\tau_{\Delta}$  may likewise not reflect changes in the solvent-dependent nonradiative deactivation term. Therefore, for a study of the effect of temperature on  $k_{\text{nr}}$ , it is prudent to avoid halogenated solvents and solvents in which  $\tau_{\Delta}$  is larger than ~5 ms.

The first experiments of any substance that revealed a systematic temperature-dependent change in  $k_{\text{nr}}$  were performed using toluene-*h*<sub>8</sub> where a subtle decrease in  $k_{\text{nr}}$  was observed over the range +60 to −50 °C (i.e.,  $\tau_{\Delta}$  change from ~27.5 to 33  $\mu\text{s}$ ).<sup>14</sup> These data yielded an apparent Arrhenius activation energy,  $E_{\text{a}}$ , for singlet oxygen deactivation of 0.84 kJ mol<sup>−1</sup>. Subsequent independent measurements yielded a slightly larger  $E_{\text{a}}$  of 1.6 ± 0.1 kJ mol<sup>−1</sup> for experiments in toluene-*h*<sub>8</sub> and  $E_{\text{a}}$  = 0.6 ± 0.4 kJ mol<sup>−1</sup> for  $\text{CH}_3\text{CN}$ .<sup>15</sup>

The available evidence thus indicated that solvent-dependent values of  $k_{\text{nr}}$  appeared to depend only weakly on temperature. When considered in light of complementary results from experiments performed using the oxygen isotopes <sup>16</sup>O<sub>2</sub> and <sup>18</sup>O<sub>2</sub>, it was concluded that, in the electronic-to-vibrational energy transfer process from singlet oxygen to the solvent, endothermic coupled transitions did not play a great role.<sup>16</sup> Rather, any temperature effects that are observed on  $k_{\text{nr}}$  must principally reflect a change in the bimolecular collision frequency.<sup>6,16</sup> Accordingly, the magnitude of a temperature dependent change in  $k_{\text{nr}}$  would scale as shown in eq 2,<sup>6</sup>

$$\frac{k_{\text{nr}}^{T_2} - k_{\text{nr}}^{T_1}}{k_{\text{nr}}^{T_2}} = \sqrt{\frac{T_2}{T_1}} - 1 \quad (2)$$

where  $k_{\text{nr}}^{T_2}$  and  $k_{\text{nr}}^{T_1}$  are the bimolecular rate constants at the temperatures  $T_2$  and  $T_1$ , respectively (given in K). In this way, a temperature change of ~80 °C over a range in which the solvent remains as a condensed liquid translates to a 10–15% change in  $k_{\text{nr}}$ . In an Arrhenius treatment, this would correspond

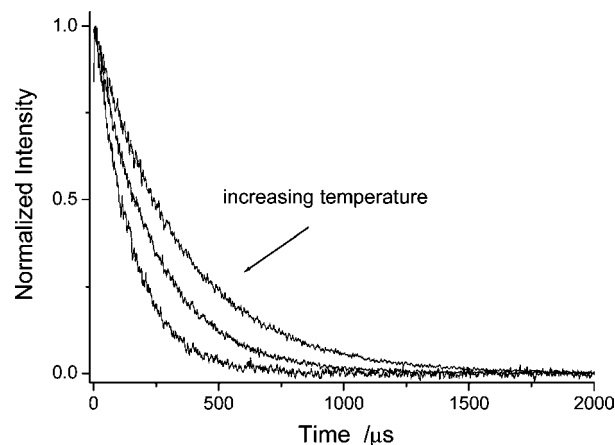


**Figure 1.** Time-resolved  $\text{O}_2(a^1\Delta_g) \rightarrow \text{O}_2(X^3\Sigma_g^-)$  phosphorescence traces recorded upon pulsed laser irradiation of the sensitizer phenaleneone in toluene-*d*<sub>8</sub>. Data shown were recorded at three different temperatures: 0.6, 31.8, and 68.4 °C.

to comparatively small apparent activation energies for solvent-dependent singlet oxygen deactivation (i.e.,  $E_{\text{a}} \sim 1$  kJ mol<sup>−1</sup>), and this was indeed consistent with the data that were available.

In the course of recent experiments in  $\text{D}_2\text{O}$ , we discovered that the solvent-dependent deactivation of singlet oxygen, in fact, appeared to have a much greater dependence on temperature than that expected on the basis of eq 2. Upon searching the literature, we discovered that our results were also consistent with a brief and apparently overlooked report of  $E_{\text{a}} = 6.7$  kJ mol<sup>−1</sup> for singlet oxygen deactivation in  $\text{D}_2\text{O}$ .<sup>17</sup> We thus set out to systematically look at a variety of solvents in order to establish a more substantive database. We now report that the solvent-dependent channel for nonradiative deactivation of singlet oxygen can indeed depend significantly on temperature in a number of common solvents, yielding apparent activation energies as large as 6–9 kJ mol<sup>−1</sup>. In the least, these results can have a number of practical ramifications in systems where singlet oxygen reactions play an important role. We also consider what these results might mean in the context of the currently accepted model of electronic-to-vibrational energy transfer for solvent-dependent singlet oxygen deactivation.

## Results

Singlet oxygen was produced upon pulsed-laser irradiation of a photosensitizer dissolved in a given solvent. In  $\text{H}_2\text{O}$  and  $\text{D}_2\text{O}$ , sulfonated phenaleneone<sup>18</sup> was used as the sensitizer, whereas phenaleneone<sup>19</sup> was used in all other solvents. The evolution of the singlet oxygen concentration was obtained by monitoring the time-resolved  $\text{O}_2(a^1\Delta_g) \rightarrow \text{O}_2(X^3\Sigma_g^-)$  phosphorescence at ~1275 nm (Figure 1). The signal decay always followed first order kinetics, thus yielding values of  $k_{\Delta}$ .

Data were recorded from six solvents and their perdeuterated complements (Table 1). Experiments were performed over a comparatively wide temperature range, limited by the freezing and boiling points of that particular solvent. To illustrate the magnitudes of the temperature-dependent changes in  $\tau_{\Delta}$ , we list in Table 1 values of  $\tau_{\Delta}$  for three temperature domains: a high temperature, room temperature, and a low temperature. The

(10) Clough, R. L.; Dillon, M. P.; Iu, K.-K.; Ogilby, P. R. *Macromolecules* **1989**, *22*, 3620–3628.

(11) Schmidt, R.; Brauer, H.-D. *J. Am. Chem. Soc.* **1987**, *109*, 6976–6981.

(12) Ogilby, P. R.; Foote, C. S. *J. Am. Chem. Soc.* **1981**, *103*, 1219–1221.

(13) Afshari, E.; Schmidt, R. *Chem. Phys. Lett.* **1991**, *184*, 128–132.

(14) Gorman, A. A.; Hamblett, I.; Lambert, C.; Spencer, B.; Standen, M. C. *J. Am. Chem. Soc.* **1988**, *110*, 8053–8059.

(15) Schmidt, R.; Seikel, K.; Brauer, H.-D. *Ber. Bunsen-Ges. Phys. Chem.* **1990**, *94*, 1100–1105.

(16) Schmidt, R.; Afshari, E. *Ber. Bunsen-Ges. Phys. Chem.* **1992**, *96*, 788–794.

(17) Rougee, M.; Bensasson, R. V. *C. R. Acad. Sci. Paris, Series II* **1986**, *302*, 1223.

(18) Nonell, S.; Gonzalez, M.; Trull, F. R. *Afinidad* **1993**, *448*, 445–450.

(19) Schmidt, R.; Tanielian, C.; Dunsbach, R.; Wolff, C. *J. Photochem. Photobiol. A: Chem.* **1994**, *79*, 11–17.

**Table 1.** Singlet Oxygen Lifetimes,  $\tau_{\Delta}$ , at High and Low Temperature Extremes and at Room Temperature<sup>a</sup>

| solvent                             | $\tau_{\Delta}^{\text{high}}/\mu\text{s}$ ( $T/^{\circ}\text{C}$ ) | $\tau_{\Delta}^{\text{RT}}/\mu\text{s}$ ( $T/^{\circ}\text{C}$ ) | $\tau_{\Delta}^{\text{low}}/\mu\text{s}$ ( $T/^{\circ}\text{C}$ ) |
|-------------------------------------|--|--|---|
| toluene- <i>h</i> <sub>8</sub>      | 26.3 (80)  | 30.3 (20)  | 31.2 (10)   |
| toluene- <i>d</i> <sub>8</sub>      | 127 (80)   | 264 <sup>b</sup> (20)  | 303 (10)  |
| benzene- <i>h</i> <sub>6</sub>      | 30.4 (75)  | 30.3 (20)  | 30.2 (10)   |
| benzene- <i>d</i> <sub>6</sub>      | 490 (75)   | 802 (20)   | 857 (10)  |
| cyclohexane- <i>h</i> <sub>12</sub> | 22.9 (75)  | 23.8 (20)  | 24.0 (10)   |
| cyclohexane- <i>d</i> <sub>12</sub> | 501 (75)   | 482 <sup>b</sup> (20)  | 478 (10)  |
| methanol- <i>h</i> <sub>4</sub>     | 10.4 (60)  | 9.8 (20)   | 9.1 (−15)   |
| methanol- <i>d</i> <sub>4</sub>     | 258 (60)   | 285 (20)   | 290 (10)  |
| CH <sub>3</sub> CN                  | 81.5 (60)  | 81.8 (20)  | 81.9 (5)  |
| CD <sub>3</sub> CN                  | 1590 (60)  | 1625 (20)  | 1635 (5)  |
| H <sub>2</sub> O                    | 3.3 (50)   | 3.5 (20)   | 3.6 (5)   |
| D <sub>2</sub> O                    | 50 (85)  | 69 (20)  | 77 (5)  |

<sup>a</sup> Errors on lifetimes are  $\sim\pm 1$ –2% of the value given. <sup>b</sup> Although these numbers agree well with what has been previously published,<sup>20</sup> they are not consistent with the established empirical rules used to calculate  $\tau_{\Delta}$  based on the energy-accepting vibrational modes in the solvent.<sup>6</sup> This could reflect a small and unknown amount of H-atom “impurity” in the solvent, or the small participation of another deactivation channel (e.g., charge transfer in the case of toluene<sup>21</sup>).

room temperature data we report are consistent with data that have been independently collected over the years.<sup>6,20</sup>

From the data in Table 1, it should be clear that in some solvents  $\tau_{\Delta}$  indeed depends negligibly on temperature (e.g., benzene-*h*<sub>6</sub>, CH<sub>3</sub>CN, cyclohexane-*h*<sub>12</sub>), whereas in other solvents (e.g., D<sub>2</sub>O, toluene-*d*<sub>8</sub>, benzene-*d*<sub>6</sub>),  $\tau_{\Delta}$  depends quite strongly on temperature. In general, the data show that  $\tau_{\Delta}$  increases with a decrease in temperature. However, for some solvents in which the temperature effect is very small (benzene-*h*<sub>6</sub>, cyclohexane-*d*<sub>12</sub> and methanol-*h*<sub>4</sub>), the opposite is observed;  $\tau_{\Delta}$  decreases with a decrease in temperature. For benzene-*h*<sub>6</sub> and cyclohexane-*d*<sub>12</sub>, the effects of a temperature-dependent change in the density of the solvent play a pronounced role in this regard and, as outlined below, it is more useful to consider values of  $k_{\text{nr}}$  rather than values of  $\tau_{\Delta}$ . The methanol-*h*<sub>4</sub> data are a bit more subtle and likely reflect a viscosity effect, as discussed in greater detail in the next section. In all cases, after recording data from a given solvent as the temperature was incremented from cold to hot, identical data were recorded from the same sample as the temperature was then decremented from hot to cold.

For all of these solvents,  $k_{\text{nr}} \gg k_{\text{r}}$ , and because (1) data were recorded in the absence of added quenchers and reactants and (2) deactivation by the photosensitizer and ground state oxygen is negligible, the temperature-dependent values of  $k_{\Delta}$  thus obtained (i.e.,  $1/\tau_{\Delta}$ ) can be directly related to the product  $k_{\text{nr}}[M]$ . For each experiment, the corresponding value of the bimolecular rate constant  $k_{\text{nr}}$  can then be obtained simply by dividing  $k_{\Delta}$  by the concentration of the solvent. For this latter operation, appropriate values of  $[M]$  were obtained using published data on temperature-dependent changes in the density of a given solvent (see Supporting Information). The resultant values of  $k_{\text{nr}}$  were then examined using an Arrhenius treatment (eq 3).

$$k_{\text{nr}} = A \exp(-E_{\text{a}}/RT) \quad (3)$$

Examples of the resultant Arrhenius plots are shown in Figure 2 (corresponding plots for the other solvents are shown in the Supporting Information). Of the 12 solvents examined, reasonably linear Arrhenius plots were obtained over a wide temperature range from seven of these solvents. Data recorded from benzene-*d*<sub>6</sub>, toluene-*d*<sub>8</sub>, methanol-*d*<sub>4</sub>, H<sub>2</sub>O, and D<sub>2</sub>O, however, yielded Arrhenius plots with a slight curvature. This is illustrated in Figure 3 for D<sub>2</sub>O and benzene-*d*<sub>6</sub> where the data are plotted on an expanded scale.

Although plots of  $\ln(k_{\text{nr}})$  against  $1/T$  readily yielded values of the apparent activation energy,  $E_{\text{a}}$ , and pre-exponential factor,  $A$ , for data from seven solvents, special measures were taken for the five solvents in which slight curvature was seen in the Arrhenius plot. Although linear fits to these latter data may not appear bad on the scale used in Figure 2 (e.g., see data for toluene-*d*<sub>8</sub>), we opted to expand the scale as shown in Figure 3 and consider the slope only in the small interval surrounding the data at room temperature, with an extrapolation of this line to yield the corresponding value of  $A$  (i.e., upon fitting a polynomial function to the data, we considered the line tangent to the curve at room temperature). Because of the potential ramifications for biologically pertinent studies, we also evaluated the tangent to the curve at 37 °C for data recorded in H<sub>2</sub>O and D<sub>2</sub>O. Clearly, for all curved Arrhenius plots, taking the slope at a point other than room temperature will yield different values of  $E_{\text{a}}$  and  $A$ . We will return to a discussion of these curved Arrhenius plots in the next section. The resultant data, for the 12 solvents examined, are listed in Table 2.

To carry our analysis further, we considered the Arrhenius data from the perspective of transition state theory to obtain values of the enthalpy and entropy of activation,  $\Delta H^{\ddagger}$  and  $\Delta S^{\ddagger}$ , respectively. In this context, we use the approximations shown in eqs 4 and 5,

$$E_{\text{a}} \approx \Delta H^{\ddagger} + RT \quad (4)$$

$$A \approx \exp(1) \frac{k_{\text{B}}T}{h} \exp(\Delta S^{\ddagger}/R) \quad (5)$$

where  $R$  is the gas constant,  $k_{\text{B}}$  is the Boltzmann constant, and  $h$  is Planck's constant.<sup>22</sup> The activation parameters thus obtained using  $T = 293$  K, and for H<sub>2</sub>O and D<sub>2</sub>O also using  $T = 310$  K, are shown in Table 2. In using eq 5, the pre-exponential factor  $A$  with the units of  $\text{M}^{-1} \text{s}^{-1}$  obtained from the Arrhenius plot was multiplied by the concentration of the given solvent at 293 K (or at 310 K) to yield a value of  $A$  with the appropriate units of  $\text{s}^{-1}$ .

## Discussion

It is clear that the solvents in which a comparatively large temperature effect on  $\tau_{\Delta}$  is observed are all perdeuterated: D<sub>2</sub>O, benzene-*d*<sub>6</sub>, toluene-*d*<sub>8</sub>, and methanol-*d*<sub>4</sub>. However, the observation of a large temperature effect on  $\tau_{\Delta}$  cannot be attributed solely to perdeuteration; only small temperature effects on  $\tau_{\Delta}$  are seen in CD<sub>3</sub>CN and cyclohexane-*d*<sub>12</sub>. Moreover, the observation of a temperature effect on  $\tau_{\Delta}$  cannot just reflect the fact that  $\tau_{\Delta}$  is comparatively long in these perdeuterated solvents; note the absence of a temperature effect in CH<sub>3</sub>CN ( $\tau_{\Delta}$  similar

(20) Wilkinson, F.; Helman, W. P.; Ross, A. B. *J. Phys. Chem. Ref. Data* **1995**, *24*, 663–1021.

(21) Darmanyan, A.; Jenks, W. S.; Jardon, P. *J. Phys. Chem. A* **1998**, *102*, 7420–7426.

(22) Laidler, K. J. *Chemical Kinetics*; 3rd ed.; Harper and Row: New York, 1987.

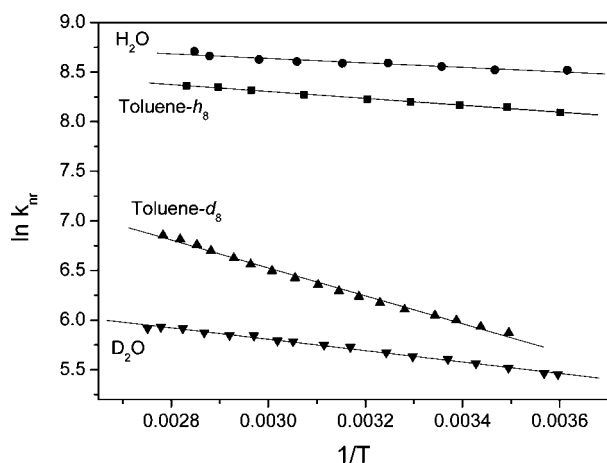


**Figure 2.** Representative Arrhenius plots for four of the solvents studied. Data for the y-axis were obtained using the bimolecular rate constant  $k_{nr}$  (i.e.,  $k_{\Delta}$  was divided by the temperature-dependent values of the solvent concentration). The solid lines are linear fits to the data.

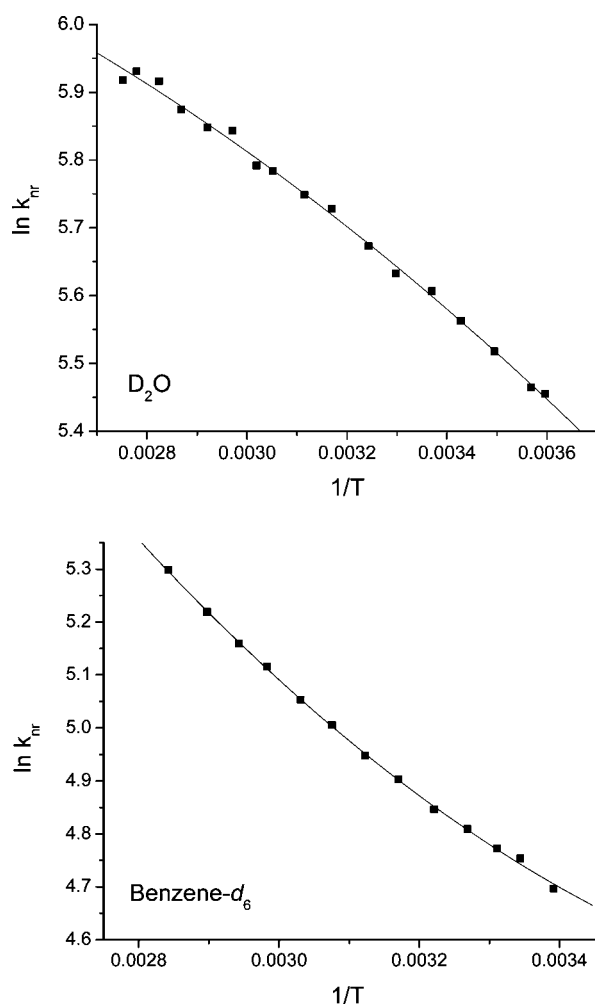


**Figure 3.** Arrhenius plots for  $k_{nr}$  data recorded from  $D_2O$  (top) and benzene- $d_6$  (bottom). The solid lines shown are the result of a polynomial fit to the data.

to that in  $D_2O$ ), in cyclohexane- $d_{12}$  ( $\tau_{\Delta}$  similar to that in benzene- $d_6$ ), or in  $CD_3CN$  (very long  $\tau_{\Delta}$ ).

For a more detailed evaluation of the data, we invoke a standard kinetic model to illustrate sequential events in the collision-dependent, solvent-induced deactivation of singlet

**Table 2.** Activation Parameters Obtained from Arrhenius plots for the Solvent-dependent Deactivation of Singlet Oxygen<sup>a</sup>

|                       | $E_a$<br>(kJ mol <sup>-1</sup> ) | $\Delta H^\ddagger$<br>(kJ mol <sup>-1</sup> ) | $A$<br>(M <sup>-1</sup> s <sup>-1</sup> ) | $A \times 10^{-3}$<br>(s <sup>-1</sup> ) | $\Delta S^\ddagger$<br>(J mol <sup>-1</sup> K <sup>-1</sup> ) | $T\Delta S^\ddagger$<br>(kJ mol <sup>-1</sup> ) |
|-----------------------|----------------------------------|--|---|--|---|---|
| toluene- $h_8$        | 2.9                              | 0.5  | 11500                                     | 110                                      | -156  | -46   |
| toluene- $d_8$        | 9.1                              | 6.7  | 17200                                     | 160                                      | -153  | -45   |
| benzene- $h_6$        | 1.0                              | -1.4   | 4500                                      | 51                                       | -163  | -48   |
| benzene- $d_6$        | 6.3                              | 3.9  | 1400                                      | 16                                       | -173  | -51   |
| cyclohexane- $h_{12}$ | 1.6                              | -0.8   | 8600                                      | 80                                       | -159  | -47   |
| cyclohexane- $d_{12}$ | 1.1                              | -1.3   | 340                                       | 3.3                                      | -186  | -55   |
| methanol- $h_4$       | -0.5                             | -2.9   | 3440                                      | 84                                       | -159  | -47   |
| methanol- $d_4$       | 2.3                              | -0.1   | 350                                       | 8.6                                      | -178  | -52   |
| $CH_3CN$              | 1.0                              | -1.4   | 985                                       | 18.7                                     | -171  | -51   |
| $CD_3CN$              | 1.6                              | -0.8   | 62  | 1.2                                      | -194  | -58   |
| $H_2O$ (at 20 °C)     | 1.2                              | -1.2   | 8420                                      | 467                                      | -145  | -42   |
| (at 37 °C)            | 1.9                              | -0.7   | 10900                                     | 604                                      | -143  | -44   |
| $D_2O$ (at 20 °C)     | 5.3                              | 2.9  | 2340                                      | 129                                      | -155  | -45   |
| (at 37 °C)            | 4.9                              | 2.5  | 1960                                      | 108                                      | -157  | -49   |

<sup>a</sup> We have opted not to put errors on the values of  $E_a$  and  $A$  simply because a significant fraction of these data were obtained from the tangent to a curved Arrhenius plot (see text). Unless otherwise specified, values of  $\Delta H^\ddagger$ ,  $\Delta S^\ddagger$ , and  $T\Delta S^\ddagger$  were obtained using a temperature of 293 K.

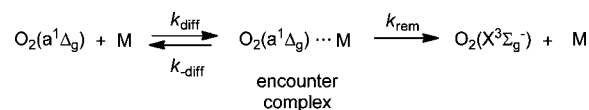


**Figure 4.** Kinetic scheme for the solvent-dependent deactivation of singlet oxygen. The letter  $M$  refers to a solvent molecule.

oxygen (Figure 4). The first step involves the diffusion-dependent encounter of singlet oxygen with a given solvent molecule to form an encounter complex. Events that occur within this encounter complex then lead to the removal of singlet oxygen from the system.

From this perspective, we can express the bimolecular rate constant obtained from our experiments,  $k_{nr}$ , as a function of the three rate constants shown in Figure 4 (eq 6).<sup>23</sup>

$$k_{nr} = \frac{k_{diff}k_{rem}}{k_{-diff} + k_{rem}} \quad (6)$$

For all solvents examined, the magnitude of  $k_{nr}$  ( $<1 \times 10^4$  s<sup>-1</sup> M<sup>-1</sup>) is characteristic of a process at the so-called pre-equilibrium limit (i.e.,  $k_{-diff} \gg k_{rem}$ ).<sup>14</sup>

Within the context of this model, one could attribute a temperature effect on  $k_{nr}$  to a number of independent phenomena. For example, one must certainly consider the contribution of temperature-dependent changes in solution viscosity; this will be manifested in the relative magnitudes of  $k_{diff}$  and  $k_{-diff}$ . Next, there is the obvious effect that temperature would have if  $k_{rem}$  quantifies an activated process (i.e., temperature defines the fraction of encounter complexes that can surmount this activation barrier to yield products). Finally, changes in temperature could independently alter the height of the barrier for the transition from the encounter complex to the products. This last effect could result from a change in the nature of the solvent in a way that is particularly pertinent for the process represented

(23) Rice, S. A. In *Comprehensive Chemical Kinetics*; Bamford, C. H., Tipper, C. F. H., Compton, R. G., Eds.; Elsevier: New York, 1985; Vol. 25, pp 1–404.



by  $k_{\text{rem}}$  which, in our case, is presumably the process of electronic-to-vibrational energy transfer. Perhaps the best example of this latter phenomenon involves water, where changes in temperature give rise to changes in the extent to which hydrogen bonding plays a role in defining the solvent system.<sup>24–26</sup>

With this perspective in mind, it is useful to think of the overall temperature effect on  $k_{\text{nr}}$  as a linear combination of independent terms, each with an appropriate weighting factor (eq 7).

$$\text{overall temperature effect on } k_{\text{nr}} = a \left[ \begin{array}{c} \text{viscosity} \\ \text{effect} \end{array} \right] + b \left[ \begin{array}{c} \text{activation} \\ \text{barrier} \end{array} \right] + c \left[ \begin{array}{c} \text{change in} \\ \text{barrier height} \end{array} \right] + \dots \quad (7)$$

At the least, the perspective represented by eq 7 could account for the curvature seen in some of the Arrhenius plots; there are a number of independent parameters that contribute to the magnitude of  $k_{\text{nr}}$ , each of which responds to temperature differently. Indeed, with this in mind, it is perhaps surprising that reasonably linear Arrhenius plots are even obtained. Thus, it is certainly appropriate to refer to an “apparent” activation energy obtained from our plots of  $\ln(k_{\text{nr}})$  against  $1/T$ .

**Viscosity Effects.** We first consider the possible effects of a temperature-dependent change in the solution viscosity (i.e., the first term in eq 7). It has previously been established that, for processes of singlet oxygen removal that occur at the pre-equilibrium limit, an increase in the viscosity of the surrounding medium causes an increase in the bimolecular rate constant for singlet oxygen removal.<sup>27,28</sup> As such, for the present experiments, if a temperature-dependent viscosity change played a significant role in influencing the data obtained, we would expect to see an increase in the magnitude of  $k_{\text{nr}}$  with a decrease in temperature. The data in Table 2 show that, for 11 of the 12 solvents examined, this is clearly not the case (i.e. the apparent activation energy,  $E_a$ , is a positive number). For these solvents,  $k_{\text{nr}}$  gets smaller with a decrease in temperature, suggesting that the process of surmounting an activation barrier must play a dominant role in events that lead to singlet oxygen removal (i.e., the second and/or third terms in eq 7 appear to be most significant).

The one possible exception to this assessment of viscosity effects involves methanol- $h_4$ , where a slightly negative value of  $E_a$  was observed. It is interesting that, for this solvent, there is nothing particularly unique about the temperature-dependent viscosity change. For a temperature change over the range 20–50 °C, the viscosity of CH<sub>3</sub>OH decreases from 570 to 394  $\mu\text{Pa s}$ .<sup>29</sup> Over the same temperature range, the viscosity of H<sub>2</sub>O, for example, decreases from 1000 to 550  $\mu\text{Pa s}$ .<sup>29</sup> Changes of similar magnitude are observed for other solvents (see Supporting Information). Thus, we can only conclude that, for CH<sub>3</sub>OH, the combination of the second and third terms in eq 7 must be small compared to the viscosity term (we elaborate

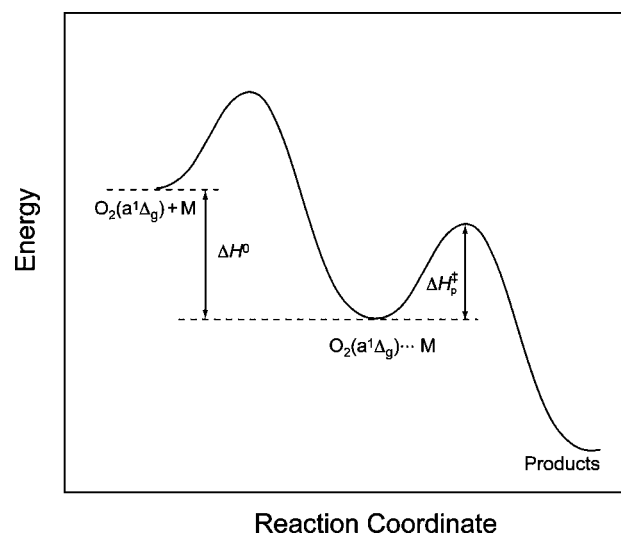


**Figure 5.** Enthalpy diagram for the deactivation of singlet oxygen by a molecule  $M$  that includes the intermediacy of a  $\text{O}_2(\text{a}^1\Delta_g)\text{-}M$  encounter complex. The potential curve is constructed to illustrate the case where the energy released upon  $\text{O}_2(\text{a}^1\Delta_g)\text{-}M$  formation,  $\Delta H^\circ$ , is larger than the activation enthalpy of product formation from the encounter complex,  $\Delta H_p^\ddagger$ . In this case, the *net* activation enthalpy,  $\Delta H^\ddagger$ , for singlet oxygen deactivation will be a negative number.

further on this point in our discussion of activation parameters, *vide infra*). In this way, the CH<sub>3</sub>OH data respond as expected on the basis of independent isothermic viscosity experiments.<sup>27,28</sup>

As an aside, and as expected, the temperature-dependent viscosity change in our solvents can manifest itself in a different way in our photosensitized singlet oxygen system. Here, we consider the encounter between the triplet state sensitizer and  $\text{O}_2(\text{X}^3\Sigma_g^-)$  that ultimately results in the production of singlet oxygen. For this process, however, the viscosity change and, independently, a temperature-dependent change in the concentration of ground-state oxygen are only important in extracting an accurate value of  $\tau_\Delta$  from H<sub>2</sub>O where the rates of singlet oxygen formation and decay are similar. This extraction of  $\tau_\Delta$  is readily achieved by fitting the time-resolved singlet oxygen phosphorescence signal to a function that also accounts for changes in the rate of singlet oxygen formation.<sup>5,30</sup>

**Activation Parameters.** Given our conclusion from the preceding section that an activation barrier must be surmounted in the process of singlet oxygen removal (i.e., that the second term in eq 7 must play an appreciable role), we now consider the activation parameters obtained from our data using eqs 4 and 5.

Within the context of the model shown in Figure 4, we first need to account for negative values of  $\Delta H^\ddagger$  (Table 2). This is readily done using an enthalpy diagram as shown in Figure 5. However, it should be noted that many of our points could also be formulated using a model that does not assume the formation of a discrete intermediate.<sup>31</sup> Nevertheless, from the perspective of structuring our discussion, and providing some continuity with the existing literature on singlet oxygen deactivation, we have opted to support our arguments starting with the diagram in Figure 5.

Progressing to the right along the reaction coordinate in Figure 5, we first show the process that corresponds to the diffusion

(24) Andersen, L. K.; Ogilby, P. R. *Rev. Sci. Instrum.* **2002**, *73*, 4313–4325.

(25) Libnau, F. O.; Toft, J.; Christy, A. A.; Kvalheim, O. M. *J. Am. Chem. Soc.* **1994**, *116*, 8311–8316.

(26) Šašić, S.; Segtnan, V. H.; Ozaki, Y. *J. Phys. Chem. A* **2002**, *106*, 760–766.

(27) Ogilby, P. R.; Dillon, M. P.; Gao, Y.; Iu, K.-K.; Kristiansen, M.; Taylor, V. L.; Clough, R. L. *Adv. Chem. Ser.* **1993**, *236*, 573–598.

(28) Scurlock, R. D.; Kristiansen, M.; Ogilby, P. R.; Taylor, V. L.; Clough, R. L. *Polym. Degrad. Stab.* **1998**, *60*, 145–159.

(29) Assael, M. J.; Polimatidou, S. K. *Int. J. Thermophys.* **1994**, *15*, 95–107.

(30) Snyder, J. W.; Skovsen, E.; Lambert, J. D. C.; Poulsen, L.; Ogilby, P. R. *Phys. Chem. Chem. Phys.* **2006**, *8*, 4280–4293.

(31) Houk, K. N.; Rondan, N. G.; Mareda, J. *Tetrahedron* **1985**, *41*, 1555–1563.

dependent formation of the  $O_2(a^1\Delta_g)-M$  encounter complex. Although we have arbitrarily shown a comparatively high activation barrier for this process, the key feature is that energy is released upon complex formation (i.e.,  $\Delta H^\circ$  is negative).

Proceeding from the  $O_2(a^1\Delta_g)-M$  complex, we then encounter a second activated process with a barrier of  $\Delta H_p^\ddagger$  to yield the products  $O_2(X^3\Sigma_g^-)$  and  $M$ . The  $\Delta H^\ddagger$  term experimentally obtained in an Arrhenius treatment is the *net* activation enthalpy for this process, and is the sum of  $\Delta H^\circ$  and  $\Delta H_p^\ddagger$ . Clearly, when  $O_2(a^1\Delta_g)-M$  complex formation is exothermic and  $|\Delta H^\circ| > |\Delta H_p^\ddagger|$ , then one obtains a negative value of  $\Delta H^\ddagger$ . It is important to note that the magnitudes of  $\Delta H^\ddagger$  involved (Table 2) are consistent with the notion that  $\Delta H^\circ$  will not be an appreciably large negative number.<sup>32–34</sup>

However, a complete description of the system must include a discussion of both enthalpy and entropy changes along the reaction coordinate. Indeed, when considered simply as a reaction profile, the enthalpy diagram shown in Figure 5 does not, by itself, conform to a situation in which a rapid and reversible pre-equilibrium is followed by a slower rate-determining step.

The Arrhenius treatment yields large negative activation entropies,  $\Delta S^\ddagger$  (Table 2). As with  $\Delta H^\ddagger$  discussed above, the values of  $\Delta S^\ddagger$  correspond to a *net* activation entropy for this multistep process. The negative sign for  $\Delta S^\ddagger$  is consistent with (1) the formation of a complex from two independently solvated species, and (2) a comparatively large amount of molecular order in the transition state to product formation. Indeed, at room temperature, values of  $T\Delta S^\ddagger$  are quite large, certainly in comparison to the values of  $\Delta H^\ddagger$ , and indicate that entropy must play a significant role in defining the reaction profile. This result is consistent with those obtained from temperature dependent studies of singlet oxygen removal using inefficient quenchers/reactants added as a solute to the system (“inefficient” in that these other processes also occur at the pre-equilibrium limit).<sup>14,35–38</sup>

In Figure 6, we again show the enthalpy diagram for a stepwise process that gives rise to a negative  $\Delta H^\ddagger$ . Superimposed on this profile is an assumed entropy profile for this process of solvent-induced singlet oxygen deactivation. Note that, along the reaction coordinate, the largest value of  $T\Delta S$  occurs at the transition state for product formation where  $O_2(a^1\Delta_g)-M$  orbital overlap is likely to be the greatest. Also shown in Figure 6 is the sum of the  $\Delta H$  and  $T\Delta S$  terms for each point along the reaction coordinate. The resultant Gibbs energy profile, and the associated Gibbs activation energies,  $\Delta G^\ddagger$ , are consistent with rate constants that characterize the pre-equilibrium limit. Specifically, such a Gibbs reaction profile indicates that the rate determining step of this two step process is indeed the second step in which the  $O_2(a^1\Delta_g)-M$  complex evolves to yield the ground state products.

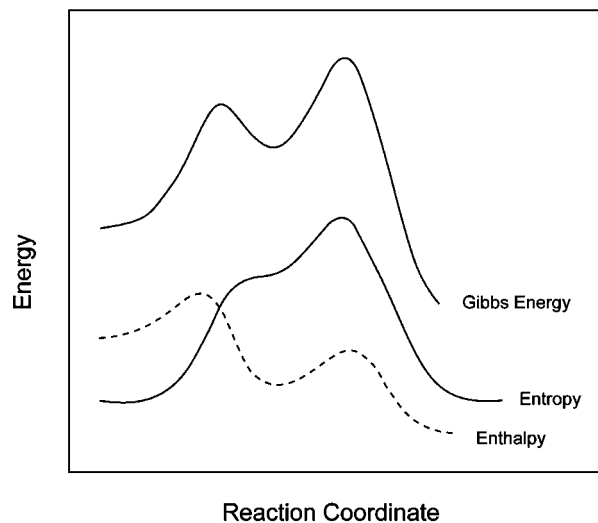


**Figure 6.** Reaction profiles for a mechanism of singlet oxygen deactivation that includes the intermediacy of a  $O_2(a^1\Delta_g)-M$  complex. The enthalpy diagram is one that results in a negative value of  $\Delta H^\ddagger$ . The assumed entropy profile corresponds both to the formation of an encounter pair from solvated reactants followed by the formation of a discrete and ordered complex as part of the electronic-to-vibrational energy transfer process. The Gibbs energy profile, obtained by adding the  $\Delta H$  and  $T\Delta S$  terms for points along the reaction coordinate, is also shown.

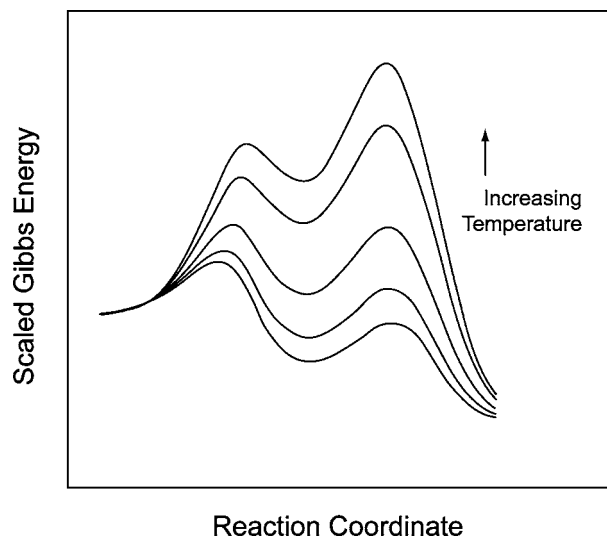


**Figure 7.** Gibbs energy profiles for a mechanism of singlet oxygen quenching by a molecule  $Q$  that includes the intermediacy of a  $O_2(a^1\Delta_g)-Q$  complex. Each curve represents the sum of the enthalpy profile shown in Figure 6 with an entropy profile scaled to represent different temperatures. For the low temperature model (bottom curve), the Gibbs energy profile corresponds to a reaction whose rate is limited by the first step in the sequence (i.e., the diffusion-controlled limit). The high-temperature model (top curve) corresponds to a reaction whose overall rate is limited by the second step in the sequence (i.e., the pre-equilibrium limit).

As an aside, and as shown in Figure 7, such reaction profiles can be used to illustrate a temperature-dependent shift from the pre-equilibrium limit (i.e.,  $k_{\text{-diff}} \gg k_{\text{rem}}$  in eq 6) to the diffusion-controlled limit (i.e.,  $k_{\text{-diff}} \ll k_{\text{rem}}$ ). Although this does not happen for the solvent-dependent singlet oxygen data shown here, it is pertinent for the removal of singlet oxygen by more efficient quenchers.<sup>14</sup>

We now consider molecule-dependent changes in the data shown in Table 2, and how the model shown in Figures 4–7 might account for these changes. For all solvents, the  $T\Delta S^\ddagger$  term

(32) Paterson, M. J.; Christiansen, O.; Jensen, F.; Ogilby, P. R. *Photochem. Photobiol.* **2006**, *82*, 1136–1160.

(33) Gooding, E. A.; Serak, K. R.; Ogilby, P. R. *J. Phys. Chem.* **1991**, *95*, 7868–7871.

(34) Khan, A. U.; Kearns, D. R. *J. Chem. Phys.* **1968**, *48*, 3272–3275.

(35) Hurst, J. R.; Wilson, S. L.; Schuster, G. B. *Tetrahedron* **1985**, *41*, 2191–2197.

(36) Bisby, R. H.; Morgan, C. G.; Hamblett, I.; Gorman, A. A. *J. Phys. Chem. A* **1999**, *103*, 7454–7459.

(37) Gorman, A. A.; Gould, I. R.; Hamblett, I.; Standen, M. C. *J. Am. Chem. Soc.* **1984**, *106*, 6956–6959.

(38) Sivaguru, J.; Solomon, M. R.; Poon, T.; Jockusch, S.; Bosio, S. G.; Adam, W.; Turro, N. J. *Acc. Chem. Res.* **2008**, *41*, 387–400.

is significantly larger than the  $\Delta H^\ddagger$  term which is consistent with an entropy-controlled process at the pre-equilibrium limit. Beyond this, there appears to be no correlation between the magnitude of  $\Delta S^\ddagger$  and the magnitude of the temperature effect on  $k_{\text{nr}}$ .

On the other hand, a reasonable correlation is observed between the magnitude of  $\Delta H^\ddagger$  and the extent to which  $k_{\text{nr}}$  depends on temperature. Specifically, solvents in which the temperature effect is pronounced yield a larger and more positive value of  $\Delta H^\ddagger$ . For these solvents, this can mean (1) formation of the  $\text{O}_2(\text{a}^1\Delta_{\text{g}})-M$  encounter complex is less exothermic than with the other solvents (i.e.,  $\Delta H^\circ$  is less negative), and/or (2) there is a larger activation enthalpy for product formation from the  $\text{O}_2(\text{a}^1\Delta_{\text{g}})-M$  complex (i.e.,  $\Delta H_{\text{p}}^\ddagger$  is more positive).

We first consider if there are obvious molecular arguments that can point to differential stabilities of the  $\text{O}_2(\text{a}^1\Delta_{\text{g}})-M$  encounter complex (i.e.,  $\Delta H^\circ$ ) that correlate with the rate data in Table 2. For the weakly bound complex between  $M$  and oxygen, it is generally considered that dispersion forces will play a significant stabilizing role.<sup>32,33</sup> From this perspective, one would expect more negative values of  $\Delta H^\circ$  for the polarizable molecules toluene and benzene. The rate data are clearly not consistent with this expectation. Alternatively, a larger amount of charge-transfer character in the  $\text{O}_2(\text{a}^1\Delta_{\text{g}})-M$  complex could likewise serve to stabilize the encounter pair and yield a more negative value of  $\Delta H^\circ$ .<sup>21,32,34,39</sup> Again, the data from toluene, for example, with its comparatively low oxidation potential, argue against this interpretation. Thus, the temperature-dependent  $k_{\text{nr}}$  data appear to derive from molecule-dependent changes in the magnitude of  $\Delta H_{\text{p}}^\ddagger$ , not  $\Delta H^\circ$ .

Our data suggest that (1) a larger value of  $\Delta H_{\text{p}}^\ddagger$  should be observed for the solvents benzene-*d*<sub>6</sub>, toluene-*d*<sub>8</sub>, and D<sub>2</sub>O, whereas (2) a smaller value of  $\Delta H_{\text{p}}^\ddagger$  should be observed for the other solvents examined. It is important to note that, with respect to methanol-*h*<sub>4</sub>, the  $\Delta H^\ddagger$  value of  $-2.9 \text{ kJ mol}^{-1}$  (Table 2) points to a value of  $\Delta H_{\text{p}}^\ddagger$  that is smaller than values of  $\Delta H_{\text{p}}^\ddagger$  obtained from the other solvents. At the least, this is consistent with our suggestion that, for CH<sub>3</sub>OH, the combination of the second and third terms in eq 7 must be small compared to the viscosity term.

Features that distinguish the group of solvents with a large value of  $\Delta H_{\text{p}}^\ddagger$  from the group of solvents with a smaller value of  $\Delta H_{\text{p}}^\ddagger$  now need to be considered in light of the currently accepted model for solvent-dependent singlet oxygen deactivation: electronic-to-vibrational energy transfer (toluene should perhaps be excluded from consideration because singlet oxygen deactivation in this solvent may include a charge-transfer-mediated process<sup>21</sup>). In the electronic-to-vibrational energy transfer model, one considers the ability of a given atom pair X-Y in the solvent molecule (e.g., O-H in water) to accept energy from singlet oxygen.<sup>6</sup> This process involves quantifying the overlap between a given energy-releasing vibronic transition in oxygen and a given energy absorbing vibrational transition in the oscillator X-Y, summed over all transitions (i.e., overtones play an important role). A great effort has been expended over the years refining aspects of this empirically derived model such that experimental data can be computationally reproduced using molecule-dependent parameters. Given these parameters, it is presently difficult to see how the inferred differences in the magnitude of  $\Delta H_{\text{p}}^\ddagger$  can be correlated to specific features of a

given molecule. Of course, as already mentioned, a key aspect in the development of this model was the notion that the electronic-to-vibrational energy transfer process did not depend appreciably on temperature. Thus, on the basis of the data reported herein, we suggest that selected parts of this model for solvent-dependent singlet oxygen deactivation need to be re-examined and further refined.

## Experimental Section

Singlet oxygen lifetimes were obtained in time-resolved experiments upon pulsed-laser excitation of a photosensitizer using an approach and instrumentation that has previously been described.<sup>40</sup> For experiments in H<sub>2</sub>O, where  $\tau_{\Delta}$  is comparatively short and  $[\text{O}_2(\text{X}^3\Sigma_{\text{g}}^-)]$  is comparatively low, it was necessary to consider the effect of temperature on the rate of singlet oxygen formation when evaluating the time-resolved  $\text{O}_2(\text{a}^1\Delta_{\text{g}}) \rightarrow \text{O}_2(\text{X}^3\Sigma_{\text{g}}^-)$  phosphorescence traces. This was accomplished using a difference of two exponential functions to fit the data.<sup>5,30</sup> Moreover, H<sub>2</sub>O data were independently recorded from air- and oxygen-saturated solutions to ensure that we were indeed properly accounting for any changes in the rate of singlet oxygen formation.

Data were recorded from air-saturated samples in a sealed 1 cm path length cuvette that, in turn, was placed in a home-built holder through which a temperature-controlled liquid could be circulated (a 1:10, by volume, mixture of ethylene glycol and water was used). A Neslab RTE-101 warming/cooling unit was used to control the temperature of this liquid. The temperature in the sample cuvette was continuously monitored by a thermometer immersed in the solvent being studied, and the samples were gently stirred during measurements. At a given temperature, recording the time-resolved singlet oxygen phosphorescence signal typically took 20–60 s. In all cases, the sensitizer absorbance at the irradiation wavelength of 400 nm was in the range 0.1–0.2.

H<sub>2</sub>O was triply distilled. Other solvents were used as received: methanol-*h*<sub>4</sub>, benzene-*h*<sub>6</sub>, cyclohexane-*h*<sub>12</sub>, toluene-*h*<sub>8</sub>, CH<sub>3</sub>CN (all from Sigma, spectroscopic grade), D<sub>2</sub>O (Euriso-Top, 99.9% D), methanol-*d*<sub>4</sub> (Euriso-Top, 99.8% D), benzene-*d*<sub>6</sub> (Euriso-Top, 99.5% D), cyclohexane-*d*<sub>12</sub> (Sigma Aldrich, 99.5% D), CD<sub>3</sub>CN (Euriso-Top, 99.8% D) and toluene-*d*<sub>8</sub> (Sigma Aldrich, 99% D). The sulfonated phenalenone was synthesized according to the method of Nonell et al.<sup>18</sup> Phenalenone (Aldrich, 97%) was recrystallized from a 2:1 mixture of CH<sub>2</sub>Cl<sub>2</sub> and CH<sub>3</sub>OH.

## Conclusions

Experiments have been performed to indicate that the solvent-specific rate constant for nonradiative deactivation of singlet oxygen can depend significantly on temperature. Given that the study of solvent-dependent singlet oxygen deactivation is a “mature” subject, it is surprising that this phenomenon has thus far escaped notice.

One of the solvents for which an appreciable temperature effect has been observed is D<sub>2</sub>O, and this can have significant ramifications for experiments examining the behavior of singlet oxygen in biologically pertinent systems. Indeed, the use of D<sub>2</sub>O instead of H<sub>2</sub>O is commonplace in many mechanistic studies of singlet oxygen, including those in live cells.<sup>5</sup> In D<sub>2</sub>O, the singlet oxygen lifetime at 37 °C is more than 10% shorter than that at room temperature (i.e.,  $k_{\text{nr}}[M]$  at 20 °C =  $1.45 \times 10^4 \text{ s}^{-1}$ ;  $k_{\text{nr}}[M]$  at 37 °C =  $1.64 \times 10^4 \text{ s}^{-1}$ ). Therefore, in aqueous media, where values of  $k_{\text{nr}}[M]$  are larger than values of  $k_{\text{q}}[Q] + k_{\text{rxn}}[R]$  for typical biologically significant processes, lowering the temperature of a given experiment from 37 to 20 °C can result in an appreciable difference in the extent to which a given

(39) Jensen, P.-G.; Arnbjerg, J.; Tolbod, L. P.; Toftegaard, R.; Ogilby, P. R. *J. Phys. Chem. A* **2009**, *113*, 9965–9973.

(40) Arnbjerg, J.; Johnsen, M.; Frederiksen, P. K.; Braslavsky, S. E.; Ogilby, P. R. *J. Phys. Chem. A* **2006**, *110*, 7375–7385.

reaction of singlet oxygen can kinetically compete with solvent deactivation. This change in relative reactivity could play an important role in studies of apoptotic cell death mediated by singlet oxygen.<sup>5</sup> Specifically, initiating the apoptotic cascade involves exceeding a threshold in the extent to which singlet oxygen reacts with intracellular components. From a different perspective, the data reported herein indicate that aspects of a well-accepted model to account for the solvent-dependent behavior of singlet oxygen need to be reconsidered. In turn, this can influence our general understanding of collision-dependent electronic-to-vibrational energy transfer in solution.

**Acknowledgment.** This work was supported by the Danish National Research Foundation.

**Supporting Information Available:** Temperature-dependent solvent density corrections; additional Arrhenius plots; singlet oxygen phosphorescence signals from H<sub>2</sub>O; temperature-dependent viscosity of the solvents examined. This material is available free of charge via the Internet at <http://pubs.acs.org>.

JA101753N